

MATTEO DEL SOLDATO ^{1*}, ADRIÁN RIQUELME ², ROBERTO TOMÁS ²,
PANTALEONE DE VITA ³ & SANDRO MORETTI ¹

APPLICATION OF STRUCTURE FROM MOTION PHOTOGRAMMETRY TO MULTI-TEMPORAL GEOMORPHOLOGICAL ANALYSES: CASE STUDIES FROM ITALY AND SPAIN

Abstract: DEL SOLDATO M., RIQUELME A., TOMÁS R., DE VITA P. & MORETTI S., *Application of Structure from Motion photogrammetry to multi-temporal geomorphological analyses: case studies from Italy and Spain*. (IT ISSN 0391-9838, 2018).

The study of the geomorphological evolution of landscapes is one of the most important tasks needed for assessing the natural and man-made geohazards and risks affecting a territory. In the last two decades, instrumental and computational advances have allowed the development of effective remote sensing methodologies, such as those based on Synthetic Aperture Radar (SAR) Interferometry or change detection techniques (Tomás & Li, 2017). These techniques have enhanced the possibilities of making geomorphic observations and modelling. Specifically, Earth Observations (EO) techniques using airborne or satellite platforms have increased the ability to map and monitor geomorphological processes. In such a framework, historical landscape data, such as those available from aerial photographs taken since the early 1940s, are key instruments for studying the geomorphological evolution of a territory.

In this work, the application of the *Structure from Motion* (SfM) technique to analyse the geomorphological evolution of sample areas by historical aerial photos is tested, examined, and discussed. Towards this aim, multi-temporal analysis by means of three-dimensional (3D) land models of four test areas reconstructed through the application of the SfM technique using available aerial images was performed. Although it is well known that SfM requires a considerable number of digital images and a significant overlap between them, the challenge of this approach

was to reconstruct 3D land models using a reduced set of analogical aerial photos for satisfactory results. The resulting 3D reconstructions succeeded in recognizing and studying the geomorphological evolution of the test areas, represented by: a) a region in southern Italy affected by landslides; b) a territory in central Italy affected by badland-type intense erosional phenomena; c) a sector in northwestern Italy with open-pit mining activity; and d) a coastal zone affected by changes in its coastline. Despite some disadvantages that arose during the application of the SfM technique, the proposed methodology has been shown to be useful for geomorphological analysis. This can be considered an alternative to the use of analogical and digital stereoscopic techniques to recognize geomorphological shapes and analyse Earth surface evolution and the effects of different anthropic activities.

KEY WORDS: Structure from Motion technique, aerial images, geomorphology, DTM reconstruction, historical data.

INTRODUCTION

In the last decades, climate change has increased the risk of extreme weather events that control geological disasters, such as landslides, erosional processes and floods, which cause related geomorphological and environmental changes. The monitoring and back-analysis of a territory play a key role in avoiding recurrences and mitigating disastrous effects, such as economic and social losses and casualties due to the occurrence of geohazards (Raspini & alii, 2018; Del Soldato & alii, 2018a; Solari & alii, 2018), which can be fostered by climate change (Crozier, 2010). During 2004-2010, more than 2,600 landslides were recorded worldwide, with over 32,000 casualties (Petley, 2012). During the same period, more than 4,700 fatal flood events were recorded, causing tens of thousands of victims (Guha-Sapir & alii, 2015). These statistics highlight the need for monitoring, mitigating, and avoiding such disastrous effects on the population and their associated economic and social impacts.

The existing approaches for the geomorphological

¹ Dipartimento di Scienze della Terra, University of Firenze, Via La Pira 4, 50121 Firenze, Italy

² Departamento de Ingeniería Civil, University of Alicante P.O. Box 99, E-03080 Alicante, Spain

³ Dipartimento di Scienze della Terra, dell'Ambiente e delle Risorse, Federico II University of Napoli, Complesso Universitario di Monte Sant'Angelo, Napoli, Italy

* Corresponding author: M. DEL SOLDATO, matteo.delsoldato@unifi.it

Part of this work was supported by the University of Alicante (vigrob-157 Project, GRE14-04 Project and GRE15-19 Project), the Spanish Ministry of Economy, Industry and Competitiveness (MINECO), the State Agency of Research (AEI) and the European Funds for Regional Development (FEDER) (projects TEC2017-85244-C2-1-P, ESP2013-47780-C2-2-R and TIN2014-55413-C2-2-P) and the Spanish Ministry of Education, Culture and Sport (project PRX17/00439).

surveying and monitoring of hazardous areas, aimed at planning or warning, can be divided into direct and indirect. Direct approaches are based on observations and/or measurements carried out by instruments in costly and time-consuming field campaigns, which allow for the collection of detailed information over areas of limited extent. Conversely, indirect approaches based on remote sensing techniques allow for the easy monitoring of geomorphological processes over wide areas with the lowest costs, even if they provide a limited resolution and a greater uncertainty. Due to the potential occurrence of hazardous and risky geomorphological processes over wide territories, remote sensing techniques can be used to investigate, map and monitor natural and man-induced processes over wide regions (Dewitte & alii, 2008; Gomez, 2014; Gomez & alii, 2015; Kjeldsen & alii, 2015, Del Soldato & alii, 2018b).

Relevant remote sensing methodologies have advanced in the last two decades due to significant technological development. The most diffused remote sensing techniques developed in the last decades are SAR (Synthetic Aperture Radar) Interferometry (Farina & alii, 2006; Ferretti & alii, 2011; Ferretti & alii, 2000; Ferretti & alii, 2001; Hooper, 2008; Hooper & alii, 2012; Massonnet & Feigl, 1998), Change Detection (Dekker, 2005; Lu & alii, 2004; Lu & alii, 2011; White, 1991), Global Positioning System (GPS) survey methods (Farolfi & alii, 2018; Brasington & alii, 2000; Brückl & alii, 2006) and terrestrial and airborne laser scanning (Niethammer & alii, 2012; Razak & alii, 2011). Moreover, in recent years, the fast-growing use of Unmanned Aerial Vehicles (UAV) has boosted the use of indirect survey techniques based on aerial photographs taken in the visible band (Niethammer & alii, 2012).

To date, geomorphological studies with aerial images, taken by on-purpose flights executed in Italy since 1943 by the Italian *Istituto Geografico Militare* (IGM), have covered almost all of the national territory with repeated campaigns and were commonly conducted by the stereoscope or developed software based on 3D computer vision algorithms (e.g., Krizhevsky & alii, 2012; Engel & alii, 2014, 2017). In Spain, several aerial survey campaigns were conducted by various agencies, and several photos are freely available on public repositories (Instituto Geográfico Nacional de España, 2016). These data consist of analogical photos, printed on photographic paper, which require stereoscopes to recognize and trace geomorphological features as well as to inspect geomorphological changes over time. These photos represent precious data sources of the past geomorphological settings for studying landscape evolution and surface processes (Carrara & alii, 2003) across several decades (Hapke, 2005). Advanced remote sensing techniques based on the use of Earth Observation (EO), such as SAR or optical products, lack the possibility of investigating historical geomorphological events that occurred before the operation of their respective satellites. To enlarge the study time span, historical analogical aerial photos can be analysed using different approaches. The first approach consists of the simple visual inspection of the available information by stereoscopes to quantitatively analyse optical images based on photogrammetric techniques (Slama & alii, 1980), which allows for the assessment of changes in topography and volumes. However, these

methods have recently been improved by the SfM technique (Fonstad & alii, 2013; Lucieer & alii, 2014; Pollefeys & alii, 1999; Westoby & alii, 2012) by means of the application of specific algorithms, even though it was originally proposed in the late 1970s (Ullman, 1979).

Non-digital aerial photos have been used by the scientific community to study the evolution of the landscape. The scope of these investigations is diverse and ranges from the study of geomorphological landscape evolution and vegetation investigations (Gomez & alii, 2015) to changes in active volcanic areas (Gomez 2014, Ishiguro & alii, 2016) and glaciers (Tonkin & alii, 2016, Mertes & alii, 2017, Mölg & Bolch, 2017), glaciological monitoring (Barrand & alii, 2009; Kjeldsen & alii, 2015; Midgley & Tonkin, 2017), land use changes (e.g. Frankl & alii, 2015), construction of Digital Surface Models (DSM) for the study of moraines (Tonkin & alii, 2014), landslide evolution and mapping (mainly developed by UAV data, e.g., Westoby & alii, 2012; Lucieer & alii, 2014; Turner & alii, 2015; Fernandez & alii, 2016; Rossi & alii, 2018) to the detection of erosion in river channels (Cook, 2017). However, historical aerial photos have not been widely applied to generate DSM and to perform the historical geomorphological analysis.

This paper explores the ability of SfM to study geomorphological evolution using reconstructions of Digital Elevation Models (DEM) from historical aerial images in different environments. Although it is well known that SfM usually requires a considerable number of highly overlapping digital images, the challenge of this work was to reconstruct multi-temporal 3D land models using a limited set of past analogical images with the recognition and retrofitting of natural Ground Control Points (GCP) to investigate the evolution of several different landscapes. The proposed methodology aims to provide an improvement from the classical use of the stereoscope to extract multitemporal geomorphological features of the territory and to recognize the potential of natural hazards while taking advantage of the cost-effective SfM approach. This approach is illustrated through four case studies: a) an area affected by a deep-seated landslide in Agnone (Molise region, southern Italy); b) a territory characterized by diffused badlands erosional processes in Atri (Abruzzo region, central Italy); c) a sector of the Graveglia valley that has important mining activities (Liguria region, northern Italy); and d) a coastal area in Portman (Murcia region, southeastern Spain).

For these four test areas, the application of the SfM technique is proposed as a valuable tool and an alternative to the classical use of stereoscopes to extract useful information about the geomorphological evolution of the territory and the recognition of potential natural hazards.

METHODS AND DATA

The methodology proposed in this work consists of the application of the SfM technique to historical aerial photos using the software Agisoft Photoscan Pro 1.2.6 build 2834 (Agisoft, 2016). The applied work-flow phases (fig. 1) and technical details of the proposed method are described below.

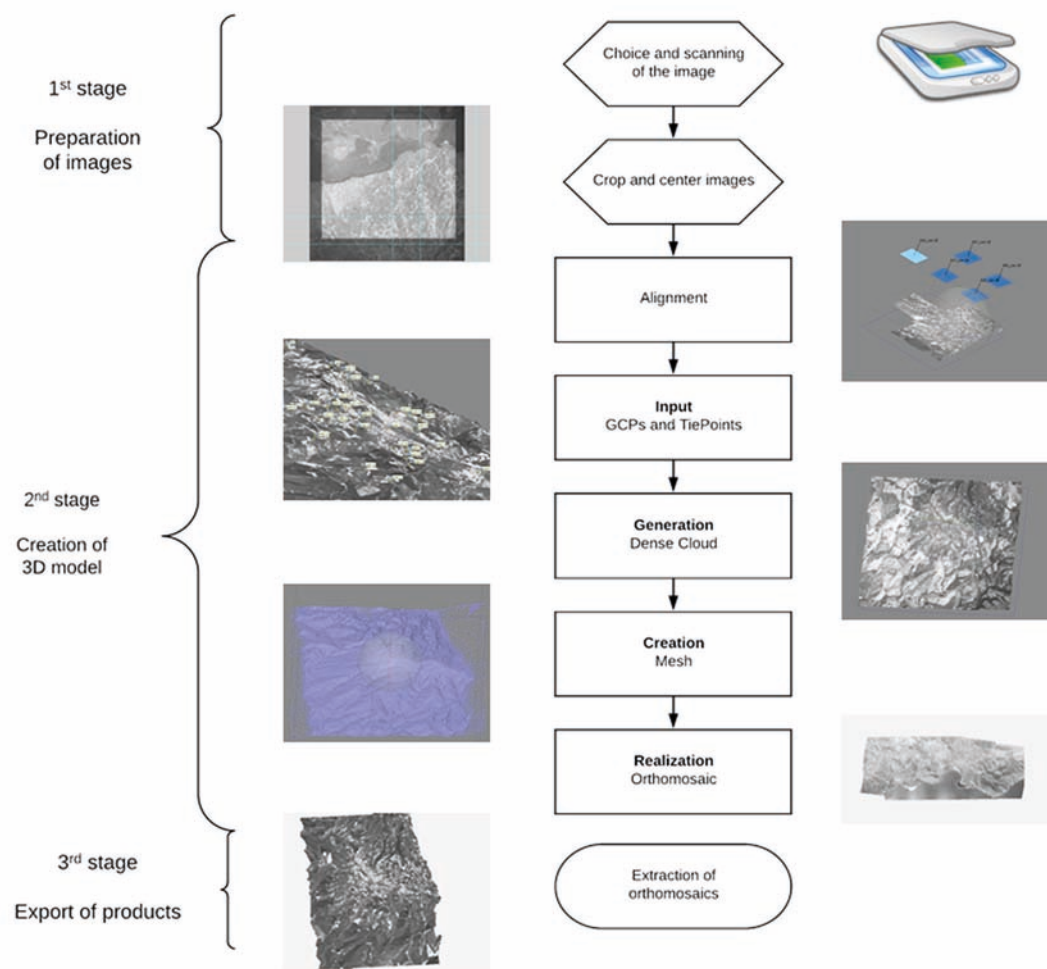


FIG. 1 - Flowchart to apply the Structure from Motion technique to a historical set of aerial images.

The first stage concerned the collection and preparation of the historical aerial analogical images, most of which are greyscale (i.e., panchromatic). To initiate the elaboration process, the aerial photos were converted into a digital format by high-quality scanning (with a high resolution of at least 600 dots per inch). During scanning, special care was taken at the four fiducial markers located at the corners of each photo, which identify the centre of the image. Keeping the centre of the digitized images is fundamental and mandatory because it represents the intersection of the visual axis with the horizontal plane crossing the flight line of the aeroplane, even when the lateral fiducial markers were removed or cropped. Additionally, it was necessary to keep the same number of pixels from picture to picture to maintain the same parameters for all images (such as the focal length), thereby allowing the software to recognize the images as shot by the same camera. Despite keeping pixel consistencies for optimal image recognition, several issues of slightly damaged images (including scratches and wear), as well as masked areas (such as military zones; fig. 2) and areas covered with clouds created some challenges for pixel matching. However, these areas were rel-

atively small (approximately 5% of the image), and therefore, they did not affect the overall DEM.

Once all images were converted into a digital format, the second stage was to load them in the Agisoft Photoscan Pro software. Subsequently, the elaboration relied on the automatic alignment of all images by estimating the internal and external camera orientation parameters in a local coordinate system using a redundant iterative bundle adjustment procedure (Snavely & alii, 2008). In addition to this estimation, all images were correlated to each other by applying only linear transformations (translation, rotation and scaling), and further elaboration stages performed non-linear transformations, which allowed the optimization of all parameters and the reconstruction of a sparse point cloud.

Then, Ground Control Points (GCP) and/or tie points, which are features visually identified in the photos with or without known coordinates in a given reference system, respectively, are inserted. Previous works have suggested that for the reconstruction of a 6 km² area, the optimal number of GPCs ranges from 20 to 25 (Barrand & alii, 2009). The insertion of these data in the elaboration process allowed

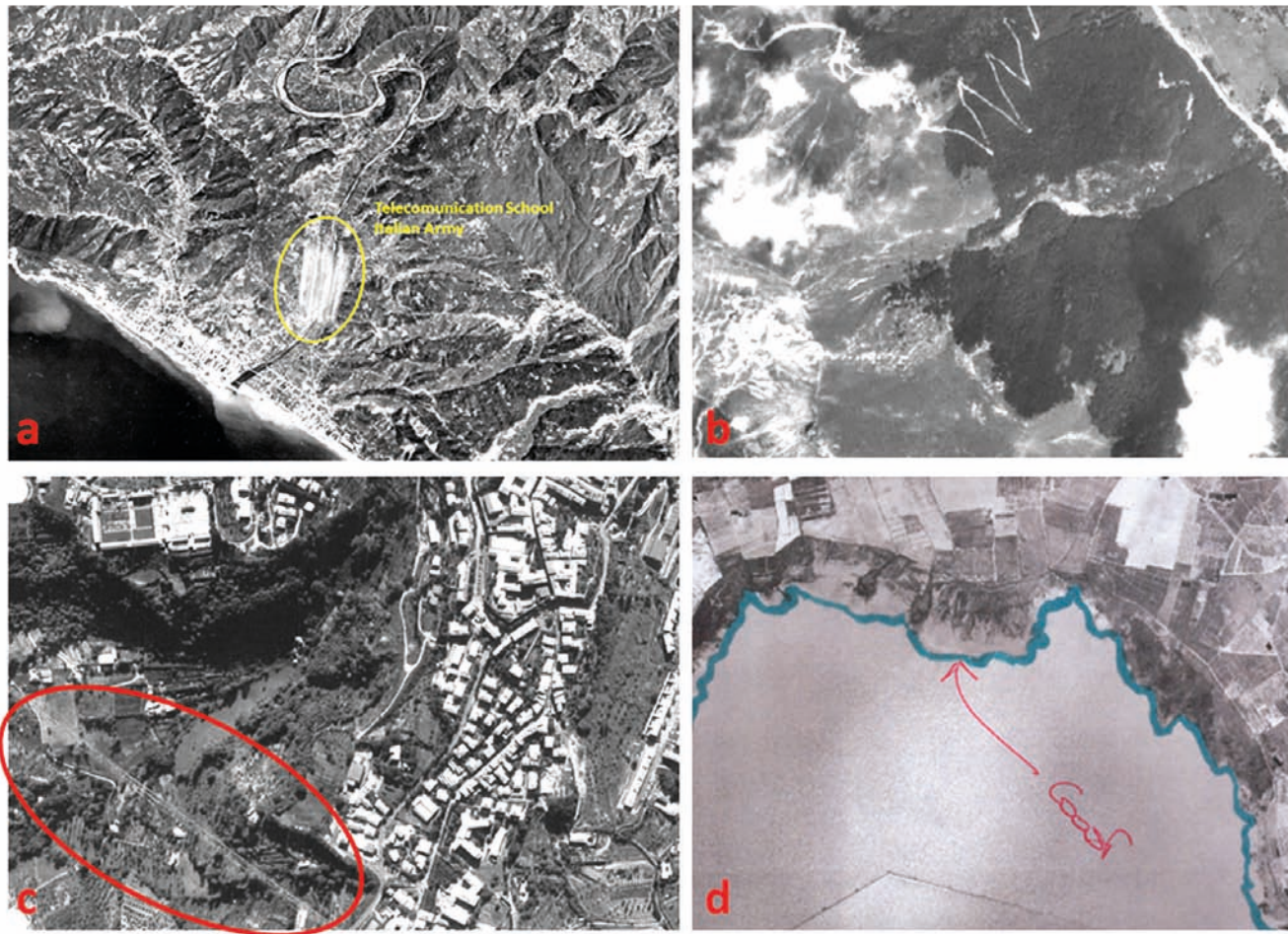


FIG. 2 - Examples of ruined historical aerial images: a) aerial photo showing an obscured area corresponding to a military facility in the Caperana municipality (Liguria, northern Italy); b) aerial image of Rigopiano hamlet in Farindola municipality (Abruzzo, central Italy) partially hidden by clouds; c) folded (red circle) aerial image from the Volterra municipality (Tuscany, central Italy); d) drawn aerial images of Salinas municipality (Alicante, southeast Spain).

scaling, orientating (with respect to geographic north and to the vertical axis) and georeferencing the 3D land models to a known geographical reference system. Moreover, the elaboration process allowed for the optimization of internal parameters to correct non-linear deformations (Barand & alii, 2009).

The fourth stage consisted of the reconstruction of a dense point cloud. At this stage, the reconstructed models were inspected to estimate the intermediate results. In the initial point cloud, empty areas (non-reconstructed areas) were found, which were determined by several factors: the presence of clouds, differences between images due to shadows, a low degree of overlap between images or even poorly textured areas (such as a water table or military crop fields).

The fifth discretionary stage resulted in the reconstruction of a mesh. This step is not mandatory because it is useful only for the previsualization of the final results and the further phase can be conducted on the dense point cloud.

In this case, a 2.5D mesh can be reconstructed due to the near-vertical acquisition of the images being unnecessary for the reconstruction of a 3D mesh. Finally, the cloud was textured by transposing and packaging the aerial photos over the elevation model and thus producing an orthomosaic image of the overlapped areas.

The precision of the GCPs coordinates was maintained as high as possible depending on i) the resolution of the scanned images and ii) the source of the coordinates of the GCPs. In the case studies proposed in this work, the insertion of precise coordinates was, in several cases, a difficult task. First, all GCPs were located in the photos with features with more relevant magnitudes (for example, crossroads, roofs of buildings or trees) to prevent loss of precision due to the image resolution. Therefore, it is reasonable to consider the use of sources of information with low resolution but relatively high precision. The coordinates and the height of the GCPs can be derived from an available DEM of the area of interest or, if it possible to conduct a

field survey, by the use of a GPS instrument, to improve the precision of the reconstruction. The data used in this work were derived from historical aerial analogical photos of the study areas and more recent DEM.

For each test area, a set of multi-temporal images was analysed and compared with more recent mono-temporal images when the images were available by means of *Web Map Services* (WMS) or Google Earth software.

In detail, the western region of the Agnone municipality test area (Molise region, southern Italy) was affected by a deep-seated landslide. This was investigated by analysing two sets of four aerial analogical panchromatic photos from 1945 and 2003, as well as considering orthophotos from 2012 derived from the WMS source data. To investigate the evolution of the erosional processes generating diffused badland landforms in the municipality of Atri (Abruzzo region, southern Italy), a series of historical aerial analogical panchromatic photos shot in 1954 were used to reconstruct a 3D land model and to compare it with recent digital satellite images. For the mining site in the Graveglia Valley (Liguria region, northern Italy), a set of seven historical aerial analogical panchromatic images shot in 1971 were used to generate the 3D land reconstruction. This was compared with a recent set of aerial photos, which represent the current geomorphological setting. Finally, the coastal

area of Portman (Murcia province, southeastern Spain) was analysed by comparing two imageries composed of six and four aerial panchromatic photos that date back to 1978 and 1984, respectively. Furthermore, orthophotos of the CNIG (*Centro Nacional de Información Geográfica*) through WMS were used to compare the reconstructed 3D land model and to identify coordinates of the GCP.

STUDY AREAS

In this section, the four case study areas are introduced. The principal characteristics of the sets of images used for reconstructing the 3D models of these areas are summarised in table 1.

Agnone landslide (Molise region, southern Italy)

The municipality of Agnone (Molise region, southern Italy) is severely affected by erosional processes and landslides. One of the most important landslides occurs in the Colle Lapponi - Piano Ovetta locality (hereafter referred to as the CL-PO landslide) (fig. 3a). In this area, an active complex deep-seated mass-movement has been recognized since the beginning of the XX century (Almagnà, 1910).

TABLE 1 - Main characteristics of the set of past analogical aerial images used for the reconstruction of 3D land models for each test area.

Site under investigation	Acquisition year	Number of aerial photos	Approximate scale	Flying height (m)	Focal length (mm)
<i>Agnone</i>	1945	4	1:55,000	7,500	137
	2003	4	1:35,000	5,300	153.31
<i>Atri</i>	1954	15	1:34,000	6,000	153.78
<i>Graveglia valley</i>	1971	7	1:26,000	4,500	152.36
<i>Portman</i>	1978	6	1:18,000	-	152.55
	1984	4	1:30,000	-	152.84

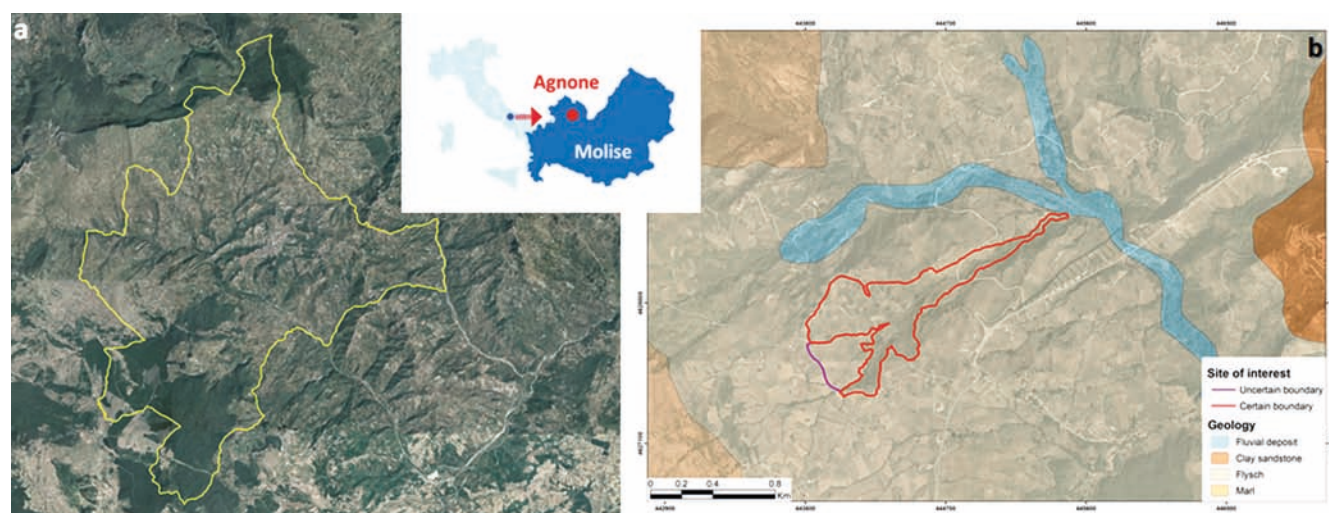


FIG. 3 - (a) Localization of the CL-PO landslide (in red) with respect to the Agnone centre (in green) and to the municipality territory (within the yellow boundary). (b) Geology of the surrounding area of the CL-PO landslide (red line).

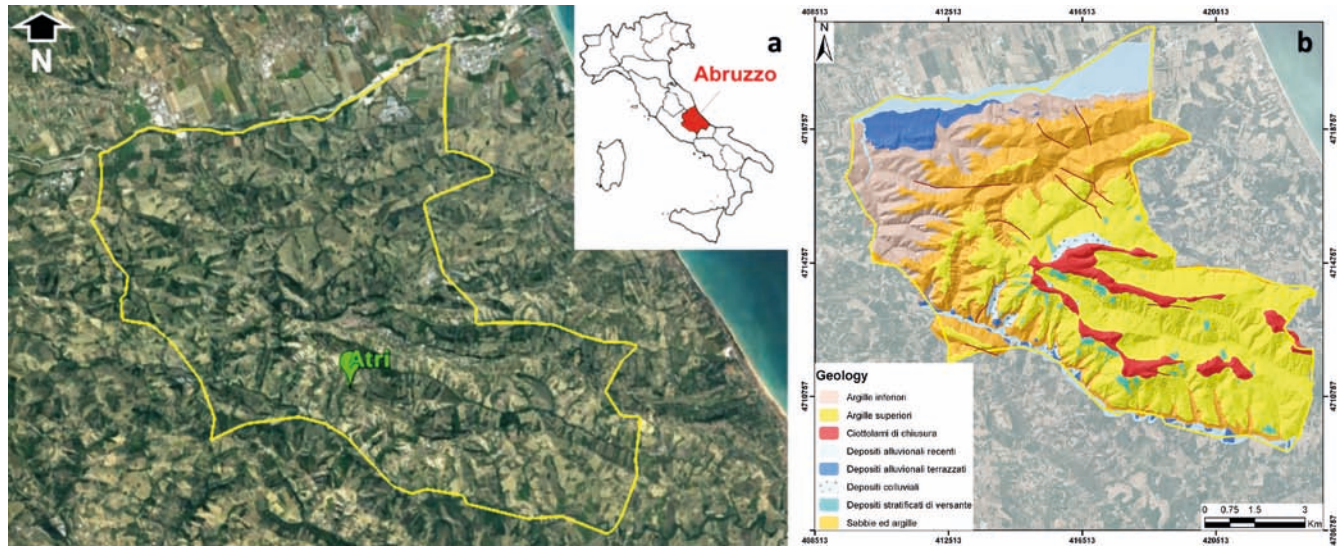


FIG. 4 - (a) Localization of the municipality of Atri. (b) Geology of the municipality of Atri.

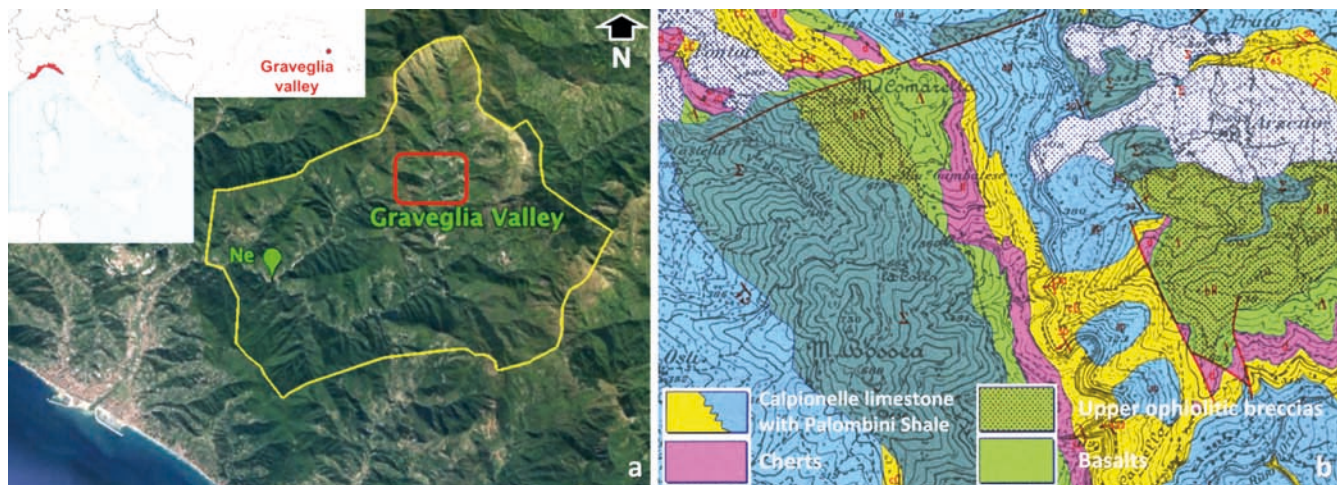


FIG. 5 - (a) Localisation of the Graveglia valley with respect to the municipality of Ne. (b) A subset of the geologic map of the Graveglia valley (from Decandia and Elter, 1972).

Recent studies allowed characterizing the mass movement with a total length of up to 1,500 m and a total volume of approximately $3.5 \times 10^6 \text{ m}^3$ (Calcaterra & alii, 2008, Del Soldato & alii, 2018a) causing important damage on structures and infrastructure (Del Soldato & alii, 2016; Del Soldato & alii, 2018c).

The landslide mainly involves the Upper Member of the Agnone Flysch (fig. 3b), which is composed of an alternation of marly and semi-coherent clays with subordinate greyish sandy levels and lithoid sandstones or calcareous intercalations with highly variable thicknesses and occasional olistoliths of conglomerates (Filocamo & alii, 2015; Vezzani & alii, 2004). Due to the lithological heterogeneity and complex structural setting, it can be considered to be a structurally complex formation (Esu, 1977). The available

historical aerial photos allowed the investigation of the geomorphological evolution of the landslide from 1945 to 2003 and up to 2012 using WMS data sources.

Atri badlands (Abruzzo region, central Italy)

The area of the municipality of Atri (Abruzzo region, central Italy) (fig. 4a) is affected by diffuse erosional processes forming particular and remarkable badlands, which control the drainage network. This territory is comprised of the peri-Adriatic belt with a geomorphological setting derived from the Mio-Pliocene evolution (Mattei & alii, 1995). The presence of Plio-Pleistocene marine sediments, representing the closing of the transitional sedimentary cycles between continental and marine depositional envi-

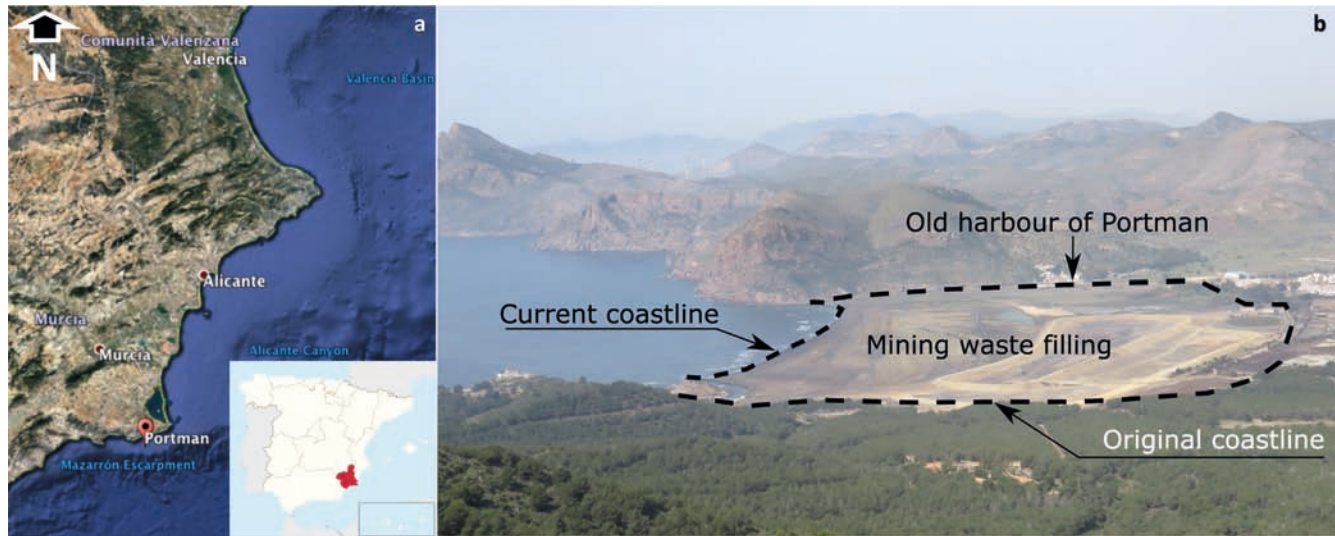


FIG. 6 - (a) Localization of the municipality of Portman and (b) general view of the Portman Bay.

ronments (Cantalamesa & Di Celma, 2004), is one of the main factors that control the badlands evolution. They are mainly characterized by clays and sands (Anselmi & alii, 1994) with cemented conglomerates at the top of the sequence (Moretti & Rodolfi, 2000). Furthermore, areas with detrital and colluvial deposits accumulated by superficial mass-movements are also recognizable (fig. 4b) in this area.

Badlands, which are commonly called “calanchi” in Italy and are widespread in several hilly clayey slopes from Tuscany to Sicily, are defined as “a heavily dissected terrain with steep, bare slopes and channels which rapidly incise and extend headwards” (Alexander, 1982). Three different types of badlands exist (Moretti & Rodolfi, 2000; Rodolfi & Frascati, 1979; Scheidegger & alii, 1968): type A, active forms featuring a V-shape with “knife-edge” landforms and a dense drainage pattern; type B, characterized by smoothed landforms and a low-intensity drainage network; and type A/B, an intermediate stage between the types A and B. Furthermore, it is possible to assess the state of activity by means of the type and density of vegetation, so far as the latter is a good indicator of the lack of active erosional processes (Buccolini & Coco, 2010; Sole & alii, 1997). Moreover, a fundamental role is played by the lithology, aspect and slope of the involved area in the badland’s evolution (Rodolfi & Frascati, 1979; Alexander, 1980; Regüés & alii, 2000; Della Seta & alii, 2007; Buccolini & alii, 2010; Buccolini & alii, 2012; Bianchini & alii, 2016).

Graveglia valley mining sites (Liguria region, northern Italy)

The third case study investigated the evolution of different mining sites located in a cropped area of the Graveglia valley in the municipality of Ne (Liguria region, northern Italy) (fig. 5a). The test area is located in the hinterland of the Tigullio coastal area, which is geologically characterized by the Ligurian oceanic series with low-grade metamorphism. Two main formations are present in the valley: the ophiolitic Bracco-Val Graveglia Unit and the Monte Gottero Unit (Brandolini & alii, 2007). The ophiolitic series of Bracco-Val Graveglia Unit is formed by (from bottom to top): serpentinites of Mt. Bossea; gabbros of Case Moggia; Mt. Capra lower ophiolitic breccias; basalt of Ponte di Lagoscurro; upper ophiolitic breccias of Monte Bianco; cherts of Mt. Roccagrande, calpionella Limestone; shale with Palombini limestone and alluvium (Abbate, 1980; Conti & Maruccci, 1991). The Mt. Gottero Unit is formed, from bottom to top, by (Brandolini & alii, 2007; Terranova, 1966): clayey and clayey-silty shales of Terisso; slates of Mt. Capenardo; marly clayey shales of Ne; sandstones of Mt. Zatta; and shales of Gaiette. In the area of interest (red box in fig. 5a), only the upper part of the ophiolitic series is present (fig. 5b).

The test area is located in the northern part of the municipality of Ne, where several historical and recent mining sites are present. In the Graveglia valley, in addition to several open pit mines at the end of the nineteenth century used to extract the manganese from the oldest pelagic cherts, additional important quarries of calcareous stones were opened in the Calpionelle limestones, which were used for concrete aggregates. Some of these quarries are still active.

Portman coastal area (southern Spain)

Portman Bay is located along the southeastern coast of Spain (fig. 6a). Its name is derived from “*Portus Magnus*” because this area was an important commercial harbour from which metal minerals (including silver-lead ore, ferric blende, pyrite and iron oxide) extracted from the Cartagena mountain range were distributed to the entire Roman Empire (Orozco & alii, 1993). More recently, from 1958 to 1991, these mining processes were modernized by a seawater flotation technique system with the capacity to process up to 10000 t day⁻¹ of pyrite (Benedicto & alii, 2008). Therefore, during this period, up to 8000 t day⁻¹ of waste

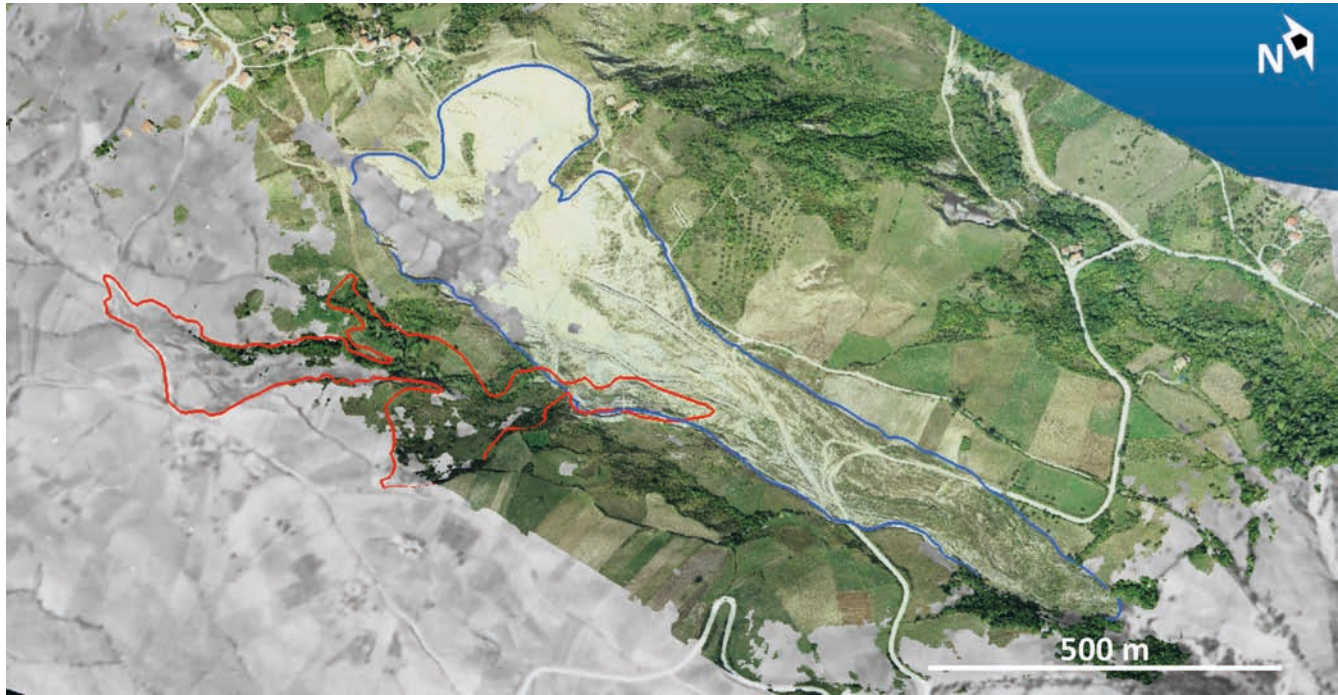


FIG. 7 - Comparison between the 3D reconstruction of the CLPO landslide applying the SfM on the historical imagery date back to 1945 (greyscale) and 2005 (colours). Red and blue contour correspond to the landslide limits mapped from 1945 and 2005 3D models, respectively.

material was directly poured into the bay, polluting an area of several kilometres (García, 2004) and accumulating more than 50 million tonnes of mine tailings (Cesar & alii, 2009) within the Portman Bay. Although this exploitation method was finally prohibited, the bay was completely filled, advancing the coastline and forming a great beach (fig. 6b).

RESULTS

Four 3D models representing different environmental frameworks were generated to investigate the geomorphological evolution of the four test areas: a) landslide-affected area in Agnone (Molise region, southern Italy); b) badlands-characterize sector of the municipality of Atri (Abruzzo region, southern Italy); c) an old mining site in the hinterland of Genoa (Liguria region, northern Italy); and d) a coastal area of Portman (Murcia region, southeastern Spain).

Agnone landslide (Molise region, southern Italy)

The 3D land model reconstructed by historical aerial photos from 1945 (fig. 7, grey image) shows an important landslide structure in the right flank of a low-order basin, causing relevant damage to a country road connecting several buildings. The comparison of 1945 and 2005 3D land models (fig. 7, colour image) shows that the right side of the basin that was affected by a landslide before 1945 has been

completely vegetated and apparently stabilized due to the effect of the drainage works carried out in the 1990s (Del Soldato & alii, 2018a). Additionally, a relevant diversion and lateral extension of the original landslide is recognizable along the left flank of the same low-order basin. The newly identified mass movement can be interpreted as an important reactivation of an older dormant landslide caused by the intense rainfalls that occurred between the 22nd and 24th of January 2003 (Calcaterra & alii, 2008). The second set of images used to reconstruct the 3D model was shot in 2005 on request by the Molise region. The analysis of both the 1945 and 2005 reconstructions permitted to trace the area involved in the landslides at these two different scenarios. Using the 3D models it was investigated the efficiency of the stabilization works performed in the left sector of the basin after the reactivation occurred in 2003. Finally, the comparison of the two 3D land models enabled to trace the boundary of the landslide in the Colle Laponi - Piano Ovetta (CL-PO) area. The 3D models also enabled the visualization by remote sensing techniques of the crack that delimits the landslide and the drainage system implemented soon after to avoid further reactivation. To monitor its recent evolution, the landslide-affected area was investigated using the InSAR technique (Del Soldato & alii, 2018a).

Atri badlands (Abruzzo region, central Italy)

Adopting the same procedure, 15 historical aerial photos from 1954 covering the territory of the Atri municipality were used to reconstruct a 3D terrain model (fig. 8a).

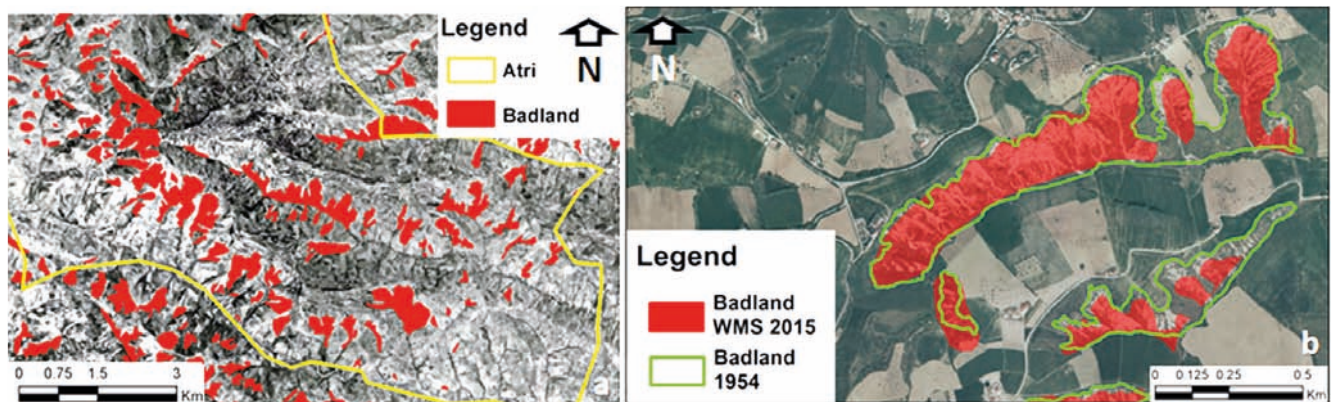


FIG. 8 - (a) 3D reconstruction from 1954 and (b) Google Earth image from 2015 of a sample area of the municipality of Atri, allowing for the comparison of the badlands inventory made on the 3D reconstruction of 1954 and the regional badlands inventory of 2015.

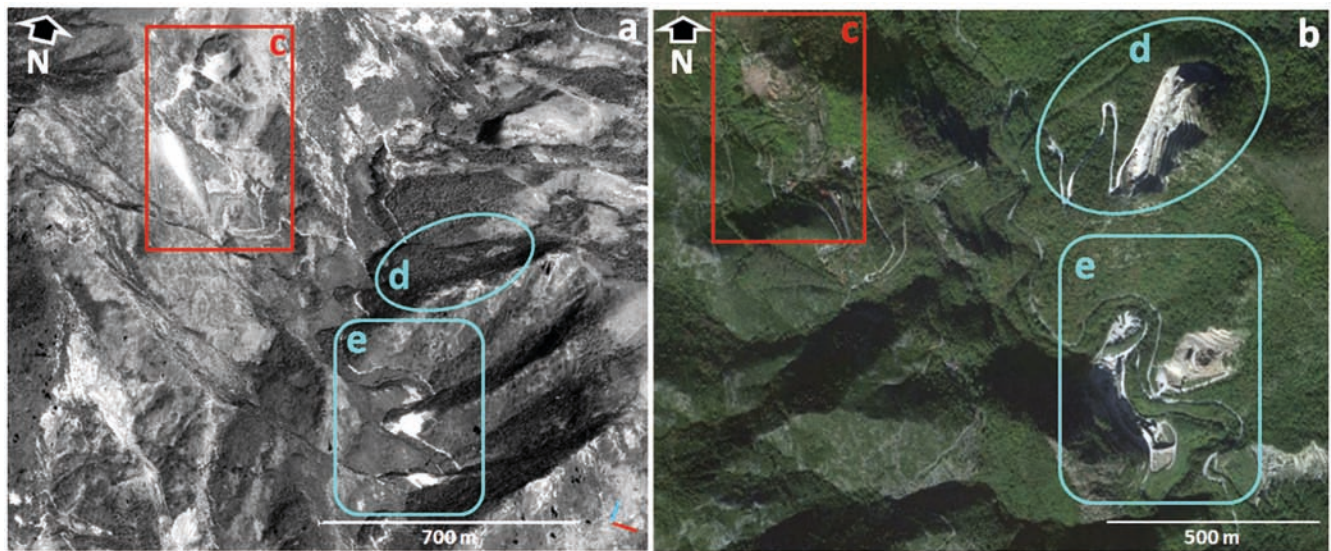


FIG. 9 - Comparison between the (a) 3D reconstruction of historical aerial images date back 1971 and (b) Google Earth images from 2015. The red “c” box is a manganese mining site, while the white boxes “d” and “e” areas show two calcareous quarries.

The analysis of the greyscale 3D land model allowed for the identification of widespread badlands shapes. The Abruzzo region made several datasets available on its website the *Web Map Service*, among which the badlands inventory was updated in 2015. The WMS was overlapped with the 3D reconstructed model from 1954 to examine the recent area in the badland with respect to the date of the reconstructed 3D model. In this way, it is possible to observe the differences between the 1954 and the most recent scenario. Several badlands, reported on the WMS maps of the Abruzzo region updated in 2015, have greater dimensions than those recognized by the 1954 3D model, with an important enlargement, while some other badlands show an increase in the vegetation cover, hiding the erosional forms and indicating a class change in their development (Moretti & Rodolfi, 2000). As an example of the continuous erosional

processes, one badland drawn on the 3D reconstruction of 1981 was compared with the inventoried eroded area from 2015, highlighting the evolution of this particular erosional shape (fig. 8b).

Graveglia valley mining sites (Liguria region, northern Italy)

In this case study, the 3D land model was reconstructed using seven available greyscale images shot in 1971 by an IGM campaign (fig. 9a).

Despite the greyscale of the 3D land model, zones affected by mining activities are easily recognisable for the lack of the vegetation and the shape of the involved area. It is interesting to notice also that different vegetation areas are recognizable: i) more thin and sparse plants in the western region and ii) a higher density of plants in the east-

ern part. The different vegetation is strictly related to the lithological features of the bedrock. The high plants reflect the Calpionelle limestone formation in the eastern sector, and the passages to the lower-density vegetation follow the contact with the red and green cherts located in the western sector. In addition, in analysing the coloured images from Google Earth dated from 2015 (fig. 9b), the change of lithology, and consequently of vegetation, is shown by the dumps of white calcareous stone (light-blue boxes d and e in fig. 9b), distinguishable with respect to the red dump of cherts (red box c in fig. 9b).

After the timespan of 45 years, important environmental modifications were recognised, chiefly caused by the

long quarrying activity carried out in the Graveglia valley. The quarrying of calcareous rocks is still active, and it is demonstrated well by two examples:

1) the light blue box d in figs. 9a and b, in which the 3D reconstruction from 1971 does not show any geomorphological form of quarry activity, in contrast to the images from 2015;

2) the light blue boxes e in figs. 9a and b show two abandoned areas from 1971 to 2015, downhill with respect to the road, which are recognizable by the dense and continuous vegetation cover, and an important development and increment of the dimension of the quarry uphill with respect to the road.

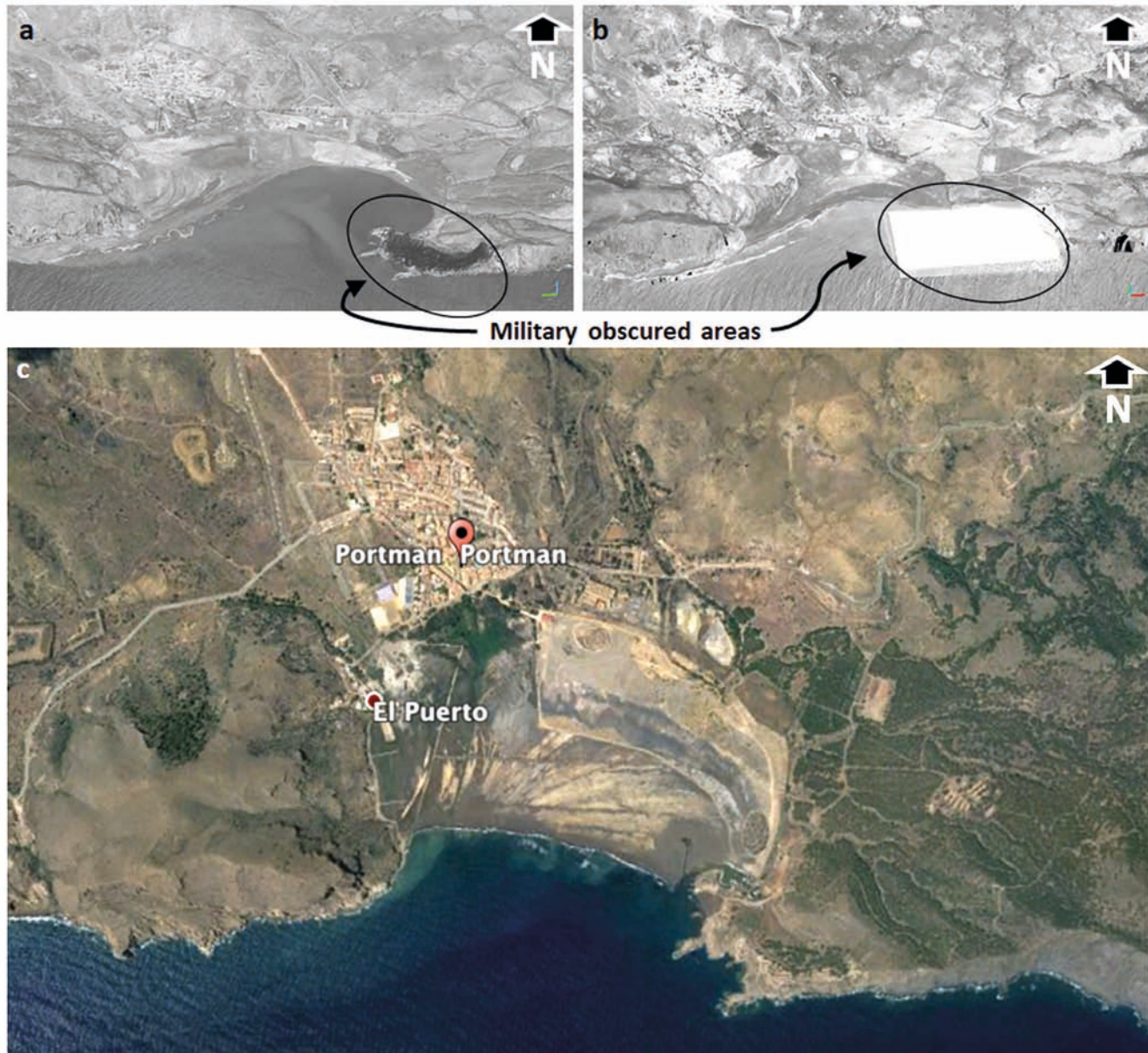


FIG. 10 - Comparison between the 3D reconstruction of the historical aerial images date back to 1971 (a), 1981 (b) and the Google Earth images from 2015 (c) of the beach of the Portman Bay, Murcia (SE Spain). Red and yellow contours represent the coastline plotted from 1981 and 2015 3D reconstructed models, respectively.

The manganese ore extraction finished in 2011, but the main important site of extraction, the Gambatesa mining site, is recognisable in both images (red box in fig. 9 a and b). Its results are more visible in the reconstructed 3D land model from 1971 by means of a big dump downhill with respect to the site and an important open pit area from which the mineral was originally extracted and from waste material that was used to fill internal voids originated during the underground extraction activities.

Portman coastal area (southern Spain)

The reconstruction of 3D land models of the Portman Bay made for 1971 (fig. 10a) and 1984 (fig. 10b) were used for the analysis of the geomorphological evolution of the coastal area. In both reconstructions, an area located on the east side of the Portman Bay is obscured because it was a military base. Although this masked area did not cause any problem during the restitution process, obviously no 3D information was obtained for this small area because the software was not able to correlate this part of the images to calculate the height and camera information.

The resulting 3D models of the area show that the bay was filled by mining waste that caused an important change in the morphology of the coastline. The 3D model derived from 1971 aerial photos (fig. 10a) shows a big gulf between two promontories, but the harbour was already captured and filled by the waste material. After ten years, in 1984 (fig. 10b), the filled area of the Gulf had increased. Finally, the Google Earth 3D model from 2015 (fig. 10c), created 24 years after the mining activity had finished, provides a clear idea of the high impact of these mining activities on the Portman Bay. Note that the local harbour (labelled “El Puerto” in Figure 10c) gives a precise idea of the position of the coastline before the filling of the bay. This impressive quantity of soils is also indicative of the mobilized material in the mining site that also provoked important geomorphological changes inland.

This case study illustrates how 3D models derived from SfM assisted in the accurate delineation of the coastline for both study periods to be compared with the present coastline shown in the 3D models available in Google Earth (fig. 10c). Additionally, the comparative analysis between the three available 3D models (i.e., the historical and Google Earth models) can also allow the operator to qualitatively or quantitatively estimate the rate of accretion (i.e., the coastal sediment returning to the visible portion of the beach) considering the accumulation of mining waste material in different time. The maximum calculated accretion velocities are approximately 20 metres per year and 6 metres per year for the periods 1971-1984 and 1984-present, respectively.

DISCUSSION AND CONCLUSIONS

The aim of this work is to show the applicability of the emergent SfM method to multi-temporal investigations of different environments in Earth studies using historical aerial analogical photos. Using the reconstruction of multi-

temporal 3D land models, the SfM technique allows for the investigation of geomorphological evolutionary stages of several natural and/or man-induced processes aimed at an advanced understanding of geohazards and risk reduction during the investigated period from 1942 and 1945, using campaigns first made by the CNIG (<http://pnoa.ign.es>) and IGM (<https://www.igmi.org>) (table 2)

In the literature, several applications of SfM have recently been published, but almost all of them have been based on imagery captured using UAVs or shot by high-resolution cameras with GPS information. Risbøl & *alii*, (2015) and Nebiker & *alii* (2014) used a similar approach to the one used in this work based on historical aerial images only to reconstruct DEM of different ages, without considering the possibility to have georeferenced orthomosaics and 3D reconstructions in which visually recognize ground fractures, scarps or other geomorphological shapes. Differently to Verhoeven & *alii* (2012), that applied SfM on aerial images for a little area for studying an archaeological site, in this manuscript the investigated area wide areas covered by different aerial images shot by camera mounted on airplane, as Frankl & *alii* (2015) made for investigating the land use changes in Ethiopia. Four different cases affected by distinct geomorphological processes were investigated using the SfM technique with panchromatic historical aerial images: a) an area involved in badland erosional phenomena; b) an area with quarrying activities; c) a coastal zone modified by the filling of mining waste; and d) a slope affected by a deep-seated landslide. These examples show that the proposed approach can be very useful for back-investigating some scenarios.

In detail, for each test area studied in this manuscript, multi-temporal 3D land models were generated by available historical aerial analogical photos. These models were used to recognize landforms and compare them with more recent data (including Google Earth images or WMS data), thus analysing different temporal stages. To achieve this goal, a procedure including the scanning of analogical images, their internal and external alignment, the building of a dense cloud, the creation of a mesh and, finally, the realization of the orthomosaic, was applied for each case study. Furthermore, for georeferencing 3D land models in a geographical coordinate system, several GCPs were identified from topographic maps or ortho-photos acquired by WMS data sources and then implemented in the models.

For each of the four case studies, the back-analysis performed by the multi-temporal 3D models allowed for the recognition of geomorphological changes from natural or man-made interventions, which could be useful for planning purposes and to promulgate mitigation measurements against disastrous recurrent geohazard events (Mili & Archarje, 2014). All of the 3D models were generated using GCPs to georeference them into a local reference system. After the reconstruction, a mesh was generated from the 3D point cloud; finally, the mesh was texturized using the scanned images. Accordingly, variously textured meshes were created. The models of each scenario enabled not only the visualisation of orthophotos but also the visual interpretation of active areas of the terrain and even the quantification of some geomorphological parameters,

TABLE 2 - Information of the available historical aerial images for the Italian and Spanish territory.

Country Organisation	Date	Number of photograms	Resolution or size of the pixel	Cost	Colour	Scale (approximate)
ITALY - IGM	1928	580	800, 2400 or 2500 dpi	Yes	Greyscale	1:33000
	1930	1088	800, 2400 or 2500 dpi	Yes	Greyscale	1:33000
	1936	17180	800, 2400 or 2500 dpi	Yes	Greyscale	1:33000
	1937	29784	800, 2400 or 2500 dpi	Yes	Greyscale	1:33000
	1940	20608	800, 2400 or 2500 dpi	Yes	Greyscale	1:33000
	1941	32252	800, 2400 or 2500 dpi	Yes	Greyscale	1:33000
	1942	12992	800, 2400 or 2500 dpi	Yes	Greyscale	1:33000
	1943	22546	800, 2400 or 2500 dpi	Yes	Greyscale	1:33000
	1944	96	800, 2400 or 2500 dpi	Yes	Greyscale	1:33000
	1945	12984	800, 2400 or 2500 dpi	Yes	Greyscale	1:33000
	1946	216	800, 2400 or 2500 dpi	Yes	Greyscale	1:33000
	1947	16385	800, 2400 or 2500 dpi	Yes	Greyscale	1:33000
	1948	16064	800, 2400 or 2500 dpi	Yes	Greyscale	1:33000
	1949	11186	800, 2400 or 2500 dpi	Yes	Greyscale	1:33000
	1950	7418	800, 2400 or 2500 dpi	Yes	Greyscale	1:33000
	1951	5063	800, 2400 or 2500 dpi	Yes	Greyscale	1:33000
	1952	7838	800, 2400 or 2500 dpi	Yes	Greyscale	1:33000
	1953	6573	800, 2400 or 2500 dpi	Yes	Greyscale	1:33000
	1954	51780	800, 2400 or 2500 dpi	Yes	Greyscale	1:33000
	1955	39724	800, 2400 or 2500 dpi	Yes	Greyscale	1:33000
	1956	2848	800, 2400 or 2500 dpi	Yes	Greyscale	1:33000
	1957	3520	800, 2400 or 2500 dpi	Yes	Greyscale	1:33000
	1958	6148	800, 2400 or 2500 dpi	Yes	Greyscale	1:33000
	1959	11316	800, 2400 or 2500 dpi	Yes	Greyscale	1:33000
	1960	7576	800, 2400 or 2500 dpi	Yes	Greyscale	1:33000
	1961	7220	800, 2400 or 2500 dpi	Yes	Greyscale	1:33000
	1962	10056	800, 2400 or 2500 dpi	Yes	Greyscale	1:33000
	1963	7316	800, 2400 or 2500 dpi	Yes	Greyscale	1:33000
	1965	18820	800, 2400 or 2500 dpi	Yes	Greyscale	1:33000
	1966	4804	800, 2400 or 2500 dpi	Yes	Greyscale	1:33000
	1967	10248	800, 2400 or 2500 dpi	Yes	Greyscale	1:33000
	1968	13212	800, 2400 or 2500 dpi	Yes	Greyscale	1:33000
	1969	13316	800, 2400 or 2500 dpi	Yes	Greyscale	1:33000
	1970	18572	800, 2400 or 2500 dpi	Yes	Greyscale	1:33000
1971	8300	800, 2400 or 2500 dpi	Yes	Greyscale	1:33000	
1972	8580	800, 2400 or 2500 dpi	Yes	Greyscale	1:33000	
1973	9660	800, 2400 or 2500 dpi	Yes	Greyscale	1:33000	
1974	27744	800, 2400 or 2500 dpi	Yes	Greyscale	1:33000	

	1975	20112	800, 2400 or 2500 dpi	Yes	Greyscale	1:33000
	1976	13884	800, 2400 or 2500 dpi	Yes	Greyscale	1:33000
	1977	7776	800, 2400 or 2500 dpi	Yes	Greyscale	1:33000
	1978	5196	800, 2400 or 2500 dpi	Yes	Greyscale	1:33000
	1979	1368	800, 2400 or 2500 dpi	Yes	Greyscale	1:33000
	1980	22208	800, 2400 or 2500 dpi	Yes	Greyscale	1:33000
	1981	12056	800, 2400 or 2500 dpi	Yes	Greyscale	1:33000
	1982	7412	800, 2400 or 2500 dpi	Yes	Greyscale	1:33000
	1983	9628	800, 2400 or 2500 dpi	Yes	Greyscale	1:33000
	1984	29664	800, 2400 or 2500 dpi	Yes	Greyscale	1:33000
	1985	27848	800, 2400 or 2500 dpi	Yes	Greyscale	1:33000
	1986	23836	800, 2400 or 2500 dpi	Yes	Greyscale	1:33000
	1987	28040	800, 2400 or 2500 dpi	Yes	Greyscale	1:33000
	1988	18404	800, 2400 or 2500 dpi	Yes	Greyscale	1:33000
	1989	18232	800, 2400 or 2500 dpi	Yes	Greyscale	1:33000
	1990	28300	800, 2400 or 2500 dpi	Yes	Greyscale	1:33000
	1991	41204	800, 2400 or 2500 dpi	Yes	Greyscale	1:33000
	1992	21624	800, 2400 or 2500 dpi	Yes	Greyscale	1:33000
	1993	13700	800, 2400 or 2500 dpi	Yes	Greyscale	1:33000
	1994	10304	800, 2400 or 2500 dpi	Yes	Greyscale	1:33000
	1995	19828	800, 2400 or 2500 dpi	Yes	Greyscale	1:33000
	1996	25060	800, 2400 or 2500 dpi	Yes	Greyscale	1:33000
	1997	18308	800, 2400 or 2500 dpi	Yes	Greyscale	1:33000
	1998	8412	800, 2400 or 2500 dpi	Yes	Greyscale	1:33000
	1999	5608	800, 2400 or 2500 dpi	Yes	Greyscale	1:33000
	2000	46928	800, 2400 or 2500 dpi	Yes	Greyscale	1:33000
	2001	2272	800, 2400 or 2500 dpi	Yes	Greyscale	1:33000
	2002	132	800, 2400 or 2500 dpi	Yes	Greyscale	1:33000
	2003	53012	800, 2400 or 2500 dpi	Yes	Greyscale	1:33000
	2004	28696	800, 2400 or 2500 dpi	Yes	Colour	1:33000
	2005	11048	800, 2400 or 2500 dpi	Yes	Colour	1:33000
	2006	564	800, 2400 or 2500 dpi	Yes	Colour	1:33000
	2010	856	800, 2400 or 2500 dpi	Yes	Colour	1:33000
Spain - CNIG	2004 - 2017	Whole Spain	0.22-0.45 m	Free	Colour	1:20000 to 1:30000
	1998-2003	Whole Spain	0.56-1 m	Free	Colour	1:40000
	1989-1991	Whole Spain	0.12 m	Free	Colour	1:50000
	1980-1986	Whole Spain	0.47-0.75 m	Free	Greyscale	1:30000
	1973-1986	Whole Spain	0.27-0.45 m	Free	Greyscale	1:18000
	1945-1946	Whole Spain	N/A	Free	Greyscale	1:43000
	1956-1957	Whole Spain	N/A	Free	Greyscale	1:32000
	1967-1968	Whole Spain	N/A	Free	Greyscale	1:45000
	1929-1930	Whole Spain	1 m	Free	Greyscale	1:10000

such as the velocity of coastline accretion. This provided a new perspective and potential when using historical aerial imagery.

In particular, analysing the CL-PO basin allowed us to highlight the potential of SfM for the exploitation of historical aerial images for landslide mapping. The old area affected by a landslide, which is currently completely vegetated, was recognized using the built 3D model from the images captured in 1945. The boundaries of the landslide, in which existing ground crack and the performed drainage works were identified was traced by means of the analysis of the 3D reconstruction developed from the 2005 imagery. For the area affected by badlands in Atri, geomorphological changes of the badlands were recognized from 1954 to 2015. The recognized modifications consisted of the retrogressing expansion and slowing down of the erosional phenomena or the growth of the vegetation in the area originally affected in 1954. Additionally, the comparison of the models allowed for the discrimination of the type of badlands (type A or type B) according to their evolution. This investigation and the derivable observations could be useful for predicting the evolution of badland areas and for defining a conscientious urban development plan. The application of the proposed methodology in the Graveglia valley shows how the back-analysis by SfM methods of historical aerial images of areas characterised by mining activity can be important for investigating the environmental and visual impact of these activities in vegetated landscapes. The comparison between the reconstruction made by historical images, even if in greyscale, against the Google Earth model allowed for recognizing the evolution of active mining sites or quarries, including the opening of new sites and their restoration or impact on the natural environment. The case study of Portman Bay shows the evolution of the coastline due to the strong contribution from the nearby mining activity that caused the accumulation of mining waste. Comparing the results obtained with the two sets of historical images and the available recent images on Google Earth 3D model, it was possible to assess the accretion of the coastal line.

Despite some disadvantages that arose during the application of the SfM technique, e.g. age and preservation of the the study shows important results for confirming the possible applications to geosciences of SfM and for historical geomorphological multitemporal analysis. The available historical greyscale images can be ruined by age, which can cause distortion and blend or alteration of the white colour of the pictures and can be further damaged if the users do not pay attention during use and dash off the surface. However, the presented case studies demonstrated that the use of these data to reconstruct georeferenced multitemporal 3D land models can be a fundamental tool for back-analysing the Earth surface evolution and analyse the effects of different natural and/or man-made process and activities in a more efficient way. Furthermore, based on the derived information, it is possible to assess future development to prevent, avoid or at least limit further social losses, economic damages or even casualties. Additionally, the 3D point clouds reconstructed for different periods could allow for the creation of precise DTM that can be

exploited for the quantitative detection of changes and the estimations of volumes (including sediment deposition and man-made excavations) over time.

In conclusion, the methodology proposed in this paper highlights the potential of SfM in the field of geosciences to exploit huge archives of available historical, greyscale and non-digital aerial images (table 2) for geomorphological multi-temporal analysis of natural and anthropogenic processes.

REFERENCES

- ABBATE E. (1980) - *Carta geologica delle ofioliti del Bargonasco e dell'Alta Val Graveglia*. Litografia Artistica Cartografica.
- AGISOFT (2016) - *Agisoft PhotoScan User Manual Professional Edition, Version 1.2*. St. Petersburg: Agisoft LLC.
- ALEXANDER D. (1980) *I calanchi-accelerated erosion in Italy*. *Geography*, 65, 95-100.
- ALEXANDER D. (1982) - *Difference between "calanchi" and "biancane" badlands in Italy*. in: BRYAN R. & YAIR A. (Eds.), *Badland Geomorphology and Piping*. Geo Books, Norwich, UK, 71-88.
- ALMAGIÀ R. (1910) - *Studi geografici sulle frane in Italia. Vol. II. L'Appennino centrale e meridionale. Conclusioni generali*. Società Geografica Italiana, 431 pp.
- ANSELMI B., CROVATO C., D'ANGELO L. & GRAUSO S. (1994) - *I calanchi di Atri (Abruzzo): caratteri mineralogici, geotecnici e geomorfologici*. *Il Quaternario*, 7 (1), 145-158.
- BARRAND N.E., MURRAY T., JAMES T.D., BARR S.L. & MILLS J.P. (2009) - *Optimizing photogrammetric DEMs for glacier volume change assessment using laser-scanning derived ground-control points*. *Journal of Glaciology*, 55, 106-116. doi: 10.3189/002214309788609001.
- BIANCHINI S., DEL SOLDATO M., SOLARI L., NOLESINI T., PRATESI F. & MORETTI S. (2016) - *Badland susceptibility assessment in Volterra municipality (Tuscany, Italy) by means of GIS and statistical analysis*. *Environmental Earth Sciences*, 75 (10), 889.
- BENEDICTO J., MARTÍNEZ-GÓMEZ C., GUERRERO J., JORNET A. & RODRÍGUEZ C. (2008) - *Metal contamination in Portman Bay (Murcia, SE Spain) 15 years after the cessation of mining activities*. *Ciencias Marinas* (2008), 34 (3), 389-398.
- BRANDOLINI P., CANEPA G., FACCINI F., ROBBIANO A. & TERRANOVA R. (2007) - *Geomorphological and Geo-Environmental Features of the Graveglia Valley (Ligurian Apennines, Italy)*. *Geografia Fisica e Dinamica Quaternaria*, 30, 99-116.
- BRASINGTON J., RUMSBY B. & MCVEY, R. (2000) - *Monitoring and modeling morphological change in a braided gravel-bed river using high resolution GPS-based survey*. *Earth Surface Processes and Landforms*, 25 (9), 973-990.
- BRÜCKL E., BRUNNER F. & KRAUS K. (2006) - *Kinematics of a deep-seated landslide derived from photogrammetric, GPS and geophysical data*. *Engineering Geology*, 88 (3), 149-159.
- BUCCOLINI M. & COCO L. (2010) - *The role of the hillside in determining the morphometric characteristics of "calanchi": the example of Adriatic central Italy*. *Geomorphology*, 123 (3), 200-210.
- BUCCOLINI M., COCO L., CAPPADONIA C. & ROTIGLIANO E. (2012) - *Relationships between a new slope morphometric index and calanchi erosion in northern Sicily, Italy*. *Geomorphology*, 149, 41-48.
- BUCCOLINI M., GENTILI B., MATERAZZI M. & PIACENTINI T. (2010) - *Late Quaternary geomorphological evolution and erosion rates in the clayey peri-Adriatic belt (central Italy)*. *Geomorphology*, 116 (1), 145-161.

- CALCATERRA D., DI MARTIRE D., RAMONDINI M., CALÒ F. & PARISE M. (2008) - *Geotechnical analysis of a complex slope movement in sedimentary successions of the southern Apennines (Molise, Italy)* in: Chen & alii (Eds.), *Landslides and Engineered Slopes*, Taylor & Francis Group, London, 299-305.
- CANTALAMESSA G. & DI CELMA C. (2004) - *Sequence response to syndepositional regional uplift: insights from high-resolution sequence stratigraphy of late Early Pleistocene strata, Periadriatic Basin, central Italy*. *Sedimentary Geology*, 164 (3), 283-309.
- CARRARA A., CROSTA G. & FRATTINI P. (2003) - *Geomorphological and historical data in assessing landslide hazard*. *Earth Surface Processes and Landforms*, 28 (10), 1125-1142.
- CESAR A., MARÍN A., MARIN-GUIRAO L., VITA R., LLORET J. & DEL VALLS T.A. (2009) - *Integrative ecotoxicological assessment of sediment in Portmán Bay (southeast Spain)*. *Ecotoxicology and environmental safety*, 72 (7), 1832-1841.
- COOK K.L. (2017) - *An evaluation of the effectiveness of low-cost UAVs and structure from motion for geomorphic change detection*. *Geomorphology* 278, 195-208. doi: 10.1016/j.geomorph.2016.11.009.
- CONTI M. & MARCUCCI M. (1991) - *Radiolarian assemblage in the Monte Alpe cherts at Ponte di Lagoscuro, Val Graveglia (eastern Liguria, Italy)*. *Eclogae Geologicae Helvetiae*, 84 (3), 791-817.
- CROZIER M. J. (2010) - *Deciphering the effect of climate change on landslide activity: A review*. *Geomorphology*, 124 (3-4), 260-267.
- DEKKER R. (2005) - *SAR change detection techniques and applications*. Munster: EARSeL.
- DELLA SETA M., DEL MONTE M., FREDI P. & PALMIERI E.L. (2007) - *Direct and indirect evaluation of denudation rates in Central Italy*. *Catena*, 71 (1), 21-30.
- DEL SOLDATO, M., DI MARTIRE, D., & TOMÁS, R. (2016) - *Comparison of different approaches for landslide-induced damage assessment: the case study of Agnone (southern Italy)*. *Rendiconti Online Società Geologica Italiana*, 41, 139-142. doi: 10.3301/ROL.2016.113.
- DEL SOLDATO M., BIANCHINI S., RIQUELME A., TOMÁS R., DE VITA P., MORETTI S. & CALCATERRA D., (2018a). *Multisource data integration to investigate one century of evolution for the Agnone landslide (Molise, southern Italy)*. *Landslides*. doi: 10.1007/s10346-018-1015-z
- DEL SOLDATO M., DEL VENTISETTE C., RASPINI F., RIGHINI G., PANCIOLI V. & MORETTI S. (2018b). *Ground deformation and associated hazards in NW Peloponnese (Greece)*. *European Journal of Remote Sensing*. doi: 10.1080/22797254.2018.1479622.
- DEL SOLDATO M., DI MARTIRE D., BIANCHINI S., TOMÁS R., DE VITA P., RAMONDINI M., CASAGLI N. & CALCATERRA D. (2018c) - *An assessment of landslide-induced damage to structures: Agnone (southern Italy) case study*. *Bulletin of Engineering Geology and the Environment*. doi: 10.1007/s10064-018-1303-9.
- ENGEL J., SCHÖPS T. & CREMERS D. (2014) - *LSD-SLAM: Large-scale direct monocular SLAM*. In: *European Conference on Computer Vision*, 834-849.
- ENGEL J., KOLTUN V. & CREMERS D. (2017) - *Direct Sparse Odometry*. *IEEE Transactions on Pattern Analysis and Machine Intelligence* 1-1. doi: 10.1109/TPAMI.2017.2658577.
- ESU F. (1977) - *Behaviour of slopes in structurally complex formations*. *Proceedings of the International Symposium on the Geotechnics of structurally complex formations*, 292-304.
- FARINA P., COLOMBO D., FUMAGALLI A., MARKS F. & MORETTI S. (2006) - *Permanent Scatterers for landslide investigations: outcomes from the ESA-SLAM project*. *Engineering Geology*, 88 (3), 200-217.
- FERNÁNDEZ T., PÉREZ J. L., CARDENAL J., GÓMEZ J. M., COLOMO C. & DELGADO J. (2016) - *Analysis of landslide evolution affecting olive groves using UAV and photogrammetric techniques*. *Remote Sensing*, 8 (10), 837.
- FERRETTI A., FUMAGALLI A., NOVALI F., PRATI C., ROCCA F. & RUCCI A. (2011) - *A new algorithm for processing interferometric data-stacks: SqueeSAR*. *IEEE Transactions on Geoscience and Remote Sensing*, 49 (9), 3460-3470.
- FERRETTI A., PRATI C. & ROCCA F. (2000) - *Nonlinear subsidence rate estimation using permanent scatterers in differential SAR interferometry*. *IEEE Transactions on Geoscience and Remote Sensing*, 38 (5), 2202-2212.
- FERRETTI A., PRATI C. & ROCCA F. (2001) - *Permanent scatterers in SAR interferometry*. *Geoscience and Remote Sensing, IEEE Transactions on*, 39 (1), 8-20.
- FILOCAMO F., ROSSKOPF C.M., AMATO V., CESARANO M. & DI PAOLA G. (2015) - *The integrated exploitation of the geological heritage: a proposal of geotourist itineraries in the Alto Molise area (Italy)*. *Rendiconti Online Società Geologica Italiana*, 33, 44-47.
- FONSTAD M.A., DIETRICH J.T., COURVILLE B.C., JENSEN J.L. & CARBONNEAU P.E. (2013) - *Topographic structure from motion: a new development in photogrammetric measurement*. *Earth Surface Processes and Landforms*, 38 (4), 421-430.
- FRANKL A., SEGHERS V., STAL C., DE MAEYER P., PETRIE G. & NYSSSEN J. (2015) - *Using image-based modelling (SfM-MVS) to produce a 1935 ortho-mosaic of the Ethiopian highlands*. *International Journal of Digital Earth*, 8 (5), 421-430.
- GARCÍA C. (2004) - *Impacto y riesgo ambiental de los residuos minerometalúrgicos de la Sierra de Cartagena-La Unión (Murcia, España)*. Ph.D. dissertation, Technical University of Cartagena, Spain.
- GOMEZ C. (2014) - *Digital photogrammetry and GIS-based analysis of the bio-geomorphological evolution of Sakurajima Volcano, diachronic analysis from 1947 to 2006*. *Journal of Volcanology and Geothermal Result*, 280, 1-13. doi: 10.1016/j.jvolgeores.2014.04.015.
- GOMEZ C., HAYAKAWA Y. & OBANAWA H. (2015) - *A study of Japanese landscapes using structure from motion derived DSMs and DEMs based on historical aerial photographs: New opportunities for vegetation monitoring and diachronic geomorphology*. *Geomorphology*, 242, 11-20. doi: 10.1016/j.geomorph.2015.02.021.
- GUHA-SAPIR D., BELOW R. & HOYOIS P. H. (2009) - *EM-DAT: The CRED/OFDA International Disaster Database* - www.emdat.be. Brussels. Belgium. Université Catholique de Louvain.
- HAPKE C. (2005) - *Estimation of regional material yield from coastal landslides based on historical digital terrain modelling*. *Earth Surface Processes and Landforms*, 30 (6), 679-697.
- HOOPER A. (2008) - *A multi-temporal InSAR method incorporating both persistent scatterer and small baseline approaches*. *Geophysical Research Letters*, 35 (16) L16302. doi:10.1029/2008GL034654.
- HOOPER A., BEKAERT D., SPAANS K. & ARIKAN M. (2012) - *Recent advances in SAR interferometry time series analysis for measuring crustal deformation*. *Tectonophysics*, 514, 1-13.
- ISHIGURO S., YAMANO H. & OGUMA H. (2016) - *Evaluation of DSMs generated from multi-temporal aerial photographs using emerging structure from motion-multi-view stereo technology*. *Geomorphology* 268, 64-71. doi:10.1016/j.geomorph.2016.05.029.
- KJELDSEN K.K., KORSGAARD N.J., BJØRK A.A., KHAN S.A., BOX J.E., FUNDER S., LARSEN N.K., BAMBER J.L., COLGAN W., VAN DEN BROEKE M., SIGGAARD-ANDERSEN M.-L., NUTH C., SCHOMACKER A., ANDRESEN C.S., WILLERSLEV E. & KJÆR K.H. (2015) - *Spatial and temporal distribution of mass loss from the Greenland Ice Sheet since AD 1900*. *Nature* 528, 396-400. doi: 10.1038/nature16183.
- KRIZHEVSKY A., SUTSKEVER I. & HINTON G.E. (2012) - *ImageNet Classification with Deep Convolutional Neural Networks*. In: PEREIRA F., BURGESS C.J.C., BOTTOU L., WEINBERGER K.Q. (Eds.), *Advances in Neural Information Processing Systems 25*. Curran Associates, Inc., 1097-1105.

- LU D., MAUSEL P., BRONDIZIO E. & MORAN E. (2004) - *Change detection techniques*. International Journal of Remote Sensing, 25 (12), 2365-2401.
- LU P., STUMPF A., KERLE N. & CASAGLI N. (2011) - *Object-oriented change detection for landslide rapid mapping*. Geoscience and Remote Sensing Letters, IEEE, 8 (4), 701-705.
- LUCIEER A., DE JONG S. & TURNER D. (2014) - *Mapping landslide displacements using Structure from Motion (SfM) and image correlation of multi-temporal UAV photography*. Progress in Physical Geography, 38 (1), 97-116. doi: 10.1177/0309133313515293.
- MASSONNET D. & FEIGL K.L. (1998) - *Radar interferometry and its application to changes in the Earth's surface*. Reviews of Geophysics, 36 (4), 441-500.
- MATTEI M., FUNICIELLO R. & KISSEL C. (1995) - *Paleomagnetic and structural evidence for Neogene block rotations in the Central Apennines, Italy*. Journal of Geophysical Research: Solid Earth, 100 (B9), 17863-17883.
- MERTES J. R., GULLEY J. D., BENN D. I., THOMPSON S. S. & NICHOLSON L. I. (2017) - *Using Structure from Motion to create Glacier DEMs and Orthoimagery from Historical Terrestrial and Oblique Aerial Imagery*. Earth Surface Processes and Landforms, 42 (14), 2350-2364. doi: 10.1002/esp.4188.
- MIDGLEY N.G. & TONKIN T.N. (2017) - *Reconstruction of former glacier surface topography from archive oblique aerial images*. Geomorphology 282, 18-26. doi:10.1016/j.geomorph.2017.01.008.
- MILI N. & ACHARJEE S. (2014) - *The Importance of Geomorphology in Understanding Natural Hazards with Special Reference to Hazards of The Dbanisiri River Basin in The Golaghat District of Assam, India*. Global Perspectives on Geography (GPG), 1-6.
- MÖLG N. & BOLCH T. (2017) - *Structure-from-Motion Using Historical Aerial Images to Analyse Changes in Glacier Surface Elevation*. Remote Sensing, 9 (10), 1021.
- MORETTI S. & RODOLFI G. (2000) - *A typical "calanchi" landscape on the Eastern Apennine margin (Atri, Central Italy): geomorphological features and evolution*. Catena, 40 (2), 217-228.
- NEBIKER S., LACK N. & DEUBER M. (2014) - *Building change detection from historical aerial photographs using dense image matching and object-based image analysis*. Remote Sensing, 6 (9), 8310-8336.
- NIETHAMMER U., JAMES M., ROTHMUND S., TRAVELLETTI J. & JOSWIG M. (2012) - *UAV-based remote sensing of the Super-Sauze landslide: Evaluation and results*. Engineering Geology, 128, 2-11.
- OROZCO J.M., HUETE F.V. & ALONZO S.G. (1993) - *Environmental problems and proposals to reclaim the areas affected by mining exploitations in the Cartagena mountains (southeast Spain)*. Landscape and Urban Planning, 23 (3-4), 195-207.
- PETLEY D. (2012) - *Global patterns of loss of life from landslides*. Geology, 40 (10), 927-930.
- POLLEFEYS M., KOCH R. & VAN GOOL L. (1999) - *Self-calibration and metric reconstruction in spite of varying and unknown intrinsic camera parameters*. International Journal of Computer Vision, 32 (1), 7-25.
- RASPINI F., BIANCHINI S., CIAMPALINI A., DEL SOLDATO M., SOLARI L., NOVALI F., DEL CONTE S., RUCCI A., FERRETTI A. & CASAGLI N. (2018) - *Continuous, semi-automatic monitoring of ground deformation using Sentinel-1 satellites*. Scientific Reports, 8.
- RAZAK K., STRAATSMAN M., VAN WESTEN C., MALET J.-P. & DE JONG S. (2011) - *Airborne laser scanning of forested landslides characterization: terrain model quality and visualization*. Geomorphology, 126 (1), 186-200.
- REGUÉS D., GUÀRDIA R. & GALLART F. (2000) - *Geomorphic agents versus vegetation spreading as causes of badland occurrence in a Mediterranean subhumid mountainous area*. Catena, 40 (2), 173-187.
- RISBØL O., BRIESE C., DONEUS M. & NESBAKKEN A. (2015) - *Monitoring cultural heritage by comparing DEMs derived from historical aerial photographs and airborne laser scanning*. Journal of Cultural Heritage, 16 (2), 202-209.
- RODOLFI G. & FRASCATI F. (1979) - *Cartografia di base per la programmazione degli interventi in aree marginali area rappresentativa dell'alta Valdera: Memorie Illustrative della Carta Geomorfologica*. Annali dell'Istituto sperimentale per la difesa del suolo, 10, 37-80.
- ROSSI G., TANTERI L., TOFANI V., VANNOCCI P., MORETTI S. & CASAGLI N. (2018) - *Multitemporal UAV surveys for landslide mapping and characterization*. Landslides, 1-8.
- SCHEIDEGGER A. SCHUMM S. & FAIRBRIDGE R. (1968) - *Badlands*. The Encyclopedia of Geomorphology, 43-48.
- SLAMA C.C., THEURER C. & HENRIKSEN S.W. [Eds.] (1980) - *Manual of photogrammetry*. American Society of photogrammetry, 1056 pp.
- SNAVELY N., SEITZ S.M. & SZELISKI R. (2008) - *Modeling the world from internet photo collections*. International Journal of Computer Vision, 80 (2), 189-210.
- SOLARI L., RASPINI F., DEL SOLDATO M., BIANCHINI S., CIAMPALINI A., FERRIGNO F., TUCCI S. & CASAGLI N. (2018) - *Satellite radar data for back-monitoring of a landslide event: the Ponzano (Central Italy) case study*. Landslides. doi: 10.1007/s10346-018-0952-x.
- SOLE A., CALVO A., CERDA A., LA R., PINI R. & BARBERO J. (1997) - *Influences of micro-relief patterns and plant cover on runoff related processes in badlands from Tabernas (SE Spain)*. Catena, 31 (1-2), 23-38.
- TERRANOVA R. (1966) - *La serie cretacea degli "Argilloscisti" fra le valli dei torrenti Entella e Petronio (Appennino Ligure)*. Atti Istituto di Geologia Università di Genova, 4 (1), 109-174.
- TOMÁS R. & LI Z. (2017) - *Earth Observations for Geohazards: Present and Future Challenges*. Remote Sensing, 9, 194. doi: 10.3390/rs9030194.
- TONKIN T.N., MIDGLEY N.G., GRAHAM D.J. & LABADZ J.C. (2014) - *The potential of small unmanned aircraft systems and structure-from-motion for topographic surveys: A test of emerging integrated approaches at Cwm Idwal, North Wales*. Geomorphology, 226, 35-43. doi:10.1016/j.geomorph.2014.07.021.
- TONKIN T.N., MIDGLEY N.G., COOK S.J. & GRAHAM D.J. (2016) - *Ice-cored moraine degradation mapped and quantified using an unmanned aerial vehicle: A case study from a polythermal glacier in Svalbard*. Geomorphology, 258, 1-10. doi:10.1016/j.geomorph.2015.12.019.
- TURNER D., LUCIEER A. & DE JONG S. M. (2015) - *Time series analysis of landslide dynamics using an unmanned aerial vehicle (UAV)*. Remote Sensing, 7 (2), 1736-1757.
- ULLMAN S. (1979) - *The interpretation of visual motion*. Proceedings of the Royal Society of London. Series B, 203, 1153, 405-426.
- VERHOEVEN G., TAELEMAN D. & VERMEULEN, F. (2012) - *Computer vision-based orthophoto mapping of complex archaeological sites: the ancient quarry of Pitaranba (Portugal-Spain)*. Archaeometry, 54 (6), 1114-1129.
- VEZZANI L., GHISETTI F., FESTA A. & FOLLADOR U. (2004) - *Carta geologica del Molise*. SELCA.
- WESTOBY M., BRASINGTON J., GLASSER N., HAMBREY M. & REYNOLDS J. (2012) - *Structure-from-Motion photogrammetry: A low-cost, effective tool for geoscience applications*. Geomorphology, 179, 300-314.
- WHITE R.G. (1991) - *Change detection in SAR imagery*. International Journal of remote sensing, 12 (2), 339-360.

(Ms. received 16 May 2017; accepted 5 July 2018)